

# First Principles Predictions of Superconductivity in Doped Stanene

Yusuf Shaidu and Omololu Akin-Ojo

*Theoretical Physics Department, African University of Science and Technology,*

*Km 10 Airport Road, Galadimawa, Abuja, Nigeria*

(Dated: June 24, 2015)

Stanene, composed of tin atoms arranged in a single layer, is the tin analogue of graphene and past studies predicted it to be a topological insulator. An energy band gap (of  $\sim 0.1$  eV) was obtained in previous calculations for the buckled honeycomb structure of stanene and, thus, phonon-mediated superconductivity in this material is ruled out. In this work we investigated, from first principles calculations within density functional theory (DFT), the possibility of producing phonon-mediated superconductivity in stanene by doping the material. It was found that doping with calcium (lithium) leads to superconductivity, albeit, with a very low superconducting transition temperature  $T_c$  of  $\sim 0.7$  K ( $\sim 1.3$  K), even lower than the value (3.7 K) for bulk  $\beta$ -Tin.

## I. INTRODUCTION

Stanene is a two dimensional sheet composed of tin (Sn) atoms arranged in a honeycomb lattice, similar to graphene. *Ab initio* calculations<sup>1</sup> indicate that, unlike graphene, a low-buckled configuration of stanene is more stable compared to the planar geometry. This is as a result of the weak  $\pi - \pi$  bonding between the atoms. The buckling enhances the overlap between  $\pi$  and  $\sigma$  orbitals and stabilizes the system.<sup>2</sup> Theoretical studies indicate that free standing stanene is a zero band gap semiconductor in the absence of spin orbit coupling (SOC). The inclusion of SOC leads to a band gap of about 0.1eV.<sup>2,3</sup> Chemical functionalization has been predicted<sup>2,3</sup> to be capable of increasing the band gap to up to 0.35 eV. With this capability of tuning its bandgap, stanene could be useful as a semiconductor in low-power-consumption electronics.

From the predicted electronic zero/non-zero band gap of stanene, one can conclude that phonon-mediated superconductivity is not possible in this material, just like its carbon counterpart graphene is not superconducting. Recently, some calculations<sup>4</sup> have, however, shown that superconductivity can be induced in graphene by n-doping at a carrier density exceeding  $10^{15} \text{ cm}^{-2}$ . Superconductivity has been produced in graphene by doping its surface with alkaline metal ad atoms.<sup>5,6</sup> This is reminiscent of the induction of superconductivity in graphite intercalated compounds (GICs).<sup>5</sup> Specifically, it was found that lithium-covered graphene has a higher superconducting transition temperature  $T_c$  than its calcium-covered counterpart unlike the situation in GICs where the opposite is the case.<sup>6</sup> Yang *et al.* showed that the superconductivity in GICs is as a result of the interaction between the interlayer (IL) states and the  $\pi^*$  states, and that, if an ad atom superlattice could be created with graphene, a similar situation could lead to superconductivity.<sup>7</sup> This was confirmed experimentally for doped graphene in Ref. 5.

With the electronic similarities between graphene and stanene, namely, the existence of a Dirac cone at the so called K point and the presence of a tunable band gap<sup>2,3</sup>, could it be possible to produce superconductivity in stanene in a manner similar to the induction of superconductivity in graphene? Doped stanene might superconduct at an even higher transition temperature  $T_c$  than doped graphene owing to the fact that bulk tin (white Tin) is superconducting at low temperatures without doping, in contrast to bulk graphene (graphite) which is not superconducting. Graphite can mainly be made superconducting by creating

interlayer states in it via metal intercalation.

To this end we examine, from first principles calculations, within Density Functional Theory (DFT), the possibility of inducing superconductivity in stanene by creating IL states in it by doping. We doped the surface of stanene with an alkaline and an alkaline earth metal, lithium and calcium, respectively and predicted  $T_c$  for these doped systems. We note that decorated stanene ( $\text{SnX}$ , with  $\text{X} = \text{OH}, \text{I}, \text{Cl}, \text{Br}$ ) have been predicted to be topological superconductors when doped with silver atoms<sup>8</sup> but the superconducting property of  $\text{SnX}$  itself was not predicted but only assumed in that study.

Stanene has recently been synthesized.<sup>9</sup> It was fabricated on a  $\text{Bi}_2\text{Te}_3(111)$  substrate by the process of molecular beam epitaxy.<sup>9</sup> This experimental realization of stanene should open up the possibility of verifying the different predictions made for the material.

## II. METHODS

We first determined the optimum structure of stanene and computed its electronic band structure. The calculations were performed using Density Functional Theory (DFT) with the gradient corrected exchange correlation functional of Perdew, Burke, and Ernzerhof (PBE).<sup>10</sup> The QUANTUM ESPRESSO<sup>11</sup> suite of codes was used. Plane waves with a kinetic energy cutoff of 55 Ry were used in expanding the wavefunctions and core electrons were excluded through the use of a norm-conserving pseudopotential.<sup>12</sup> We inserted a vacuum layer with a width larger than  $20\text{\AA}$  in the non-periodic direction of the system. Since the material under consideration is a semimetal, the electronic properties were determined by integration in the first Brillouin zone (BZ) using a Gaussian smearing having a width of 0.05 Ry. All configurations and their respective atomic positions were optimized ensuring that the maximum force on any atom was smaller than  $10^{-4}\text{eV/\AA}$ . The electronic band structure was calculated along the path connecting the special high symmetry k-points  $\Gamma, M, K$  in the first BZ as shown in Sect. III below. The electronic density of states (EDOS) was computed using a finer mesh of the first BZ with electron momentum of  $27 \times 27 \times 1$  and  $21 \times 21 \times 1$  for stanene, and doped stanene respectively.

Next, the phonon band structure and phonon density of states (PDOS) were calculated in the framework of density functional perturbation theory (DFPT) as implemented in the QUANTUM ESPRESSO codes.<sup>13</sup> These calculations showed, among other things, the sta-

bility of the buckled stanene structure. The electron-phonon coupling (EPC) constants  $\lambda$  were also determined but only for doped stanene since undoped stanene does not superconduct. The necessary summations over the electron momenta and phonon momenta (see Eqs. 4 and 5 below) in computing the EPC constants were carried out using an electron momentum mesh of  $32 \times 32 \times 1$  and a phonon momentum one of  $8 \times 8 \times 1$ .

We used the following formula by Allen and Dynes<sup>14</sup> to determine the superconducting transition temperature  $T_c$ :

$$T_c = \frac{\omega_{log}}{1.20} \exp \left( -\frac{1.04(1 + \lambda)}{\lambda - \mu^*(1 + 0.62\lambda)} \right), \quad (1)$$

where,  $\omega_{log}$ ,  $\lambda$  and  $\mu^*$  are the logarithmic average of the phonon energy, electron-phonon coupling constant and the electron-electron Coulomb repulsion parameter, respectively. The first two quantities were calculated as:

$$\omega_{log} = \exp \left( \frac{2}{\lambda} \int_0^\infty \alpha^2 F(\omega) \ln \omega \frac{d\omega}{\omega} \right) \quad (2)$$

$$\lambda = 2 \int_0^\infty \frac{\alpha^2(\omega) F(\omega)}{\omega} d\omega \quad (3)$$

where, the Eliashberg function  $\alpha^2 F$  is given by

$$\alpha^2 F(\omega) = \frac{1}{N(0)N_{\mathbf{k}}N_{\mathbf{k}'}} \sum_{\mathbf{k}, \mathbf{k}', v} |M_{\mathbf{k}, \mathbf{k}'}^\nu|^2 \delta(\epsilon_{\mathbf{k}}) \delta(\epsilon_{\mathbf{k}'}) \delta(\omega - \omega_{\mathbf{q}, \nu}). \quad (4)$$

The terms that appear in the expression are defined as follows:  $N(0)$  is the electronic density of states per spin at the Fermi level, i.e.,  $N(0) = \sum_{\mathbf{k}} \delta(\epsilon_{\mathbf{k}})$  and  $N_{\mathbf{k}}$  and  $N_{\mathbf{q}}$  represent the total number of  $\mathbf{k}$  and  $\mathbf{q}$  points respectively. The Kohn-Sham eigenvalue with reference to the Fermi level is  $\epsilon_k$  and  $M_{k, k'}$  is the electron-phonon coupling matrix element. The Dirac delta distributions  $\delta(\epsilon_{\mathbf{k}})$  and  $\delta(\epsilon_{\mathbf{k}'})$  restrict the electrons to the Fermi surface,  $\omega_{\mathbf{q}, \nu}$  is the phonon frequency at the phonon wave vector  $\mathbf{q}$  of the phonon branch of index  $\nu$ . Here,  $k$  and  $k'$  indicate both the electron wave vector and band index, and spin index.  $\mathbf{q} = \mathbf{k}' - \mathbf{k}$  indicates both the phonon wave vector and band index. In our calculations the Dirac delta distribution of Eq. 4 above was replaced by a Gaussian broadening function having a width of 0.01 Ry. The variable  $\alpha^2$  is the coupling strength and  $F(\omega)$  is the phonon density of state,

i.e.,

$$F(\omega) = \sum_{\mathbf{q}} \delta(\omega - \omega_{\mathbf{q}}) \quad (5)$$

### III. RESULTS AND DISCUSSION

The optimized lattice parameters are shown in Table I along with the results obtained from calculations in the Literature. The variable  $a$  is the lattice constant,  $d$  is the out-of-plane buckled height, and  $a_{sn-sn}$  is the Sn–Sn bond length. The values calculated in this work are consistent with other theoretical predictions in the literature. We also found the buckled stanene structure to be stable. The computed phonon band structure of pristine stanene had no imaginary frequency. This stability is in agreement with Ref. 2,3 but differs from the results presented in the supplementary information of Ref. 15.

Next, we present the electronic band structure and the electronic density of states of free standing stanene. The band structure and the density of states in Fig.2 are in good agreement with the results of Broek *et al.*<sup>3</sup> The figure clearly shows that stanene has a Dirac point at K similar to the case in graphene. Thus, it is a zero band gap material. Our calculations did not include spin-orbit coupling (SOC) effects. It is known that SOC opens up the gap by about 0.1 eV at the K point. In either case, with or without SOC, the electron density at the Fermi level is very low for stanene. Consequently, free-standing stanene cannot superconduct due to a lack of carriers at the Fermi level that can participate in Cooper pairing.

A first attempt towards making stanene a superconductor is to assume phonon mediated superconductivity and mimic the way in which its two dimensional counterpart, graphene was made superconducting as reported in Refs. 5,7,16. Hence we doped stanene with an electron donor, in this case with Lithium and Calcium, respectively, in order to create an electron rich Fermi surface. Electrons at the Fermi surface can then form Cooper pairs and make the material superconducting.

We placed Lithium atoms and Calcium atoms in turn on stanene as shown in Fig. 1 and optimized the resulting structures but with the fixed lattice constant ( $a = 4.64 \text{ \AA}$ ) obtained for free-standing stanene. The optimized structure of Lithium (Calcium) doped stanene reveals that the structure is stable when Lithium (Calcium) atoms were placed at 1.75 (2.24)  $\text{\AA}$  above the stanene plane. No imaginary frequencies were seen in the computed

phonon dispersion curves (see Fig. 5).

The electronic band structures of Lithium-doped and Calcium-doped stanene are shown in Fig. 4. From the figure, it is clear that carriers are now available near the Fermi surface in contrast to the situation with free-standing stanene (Fig. 2).

### A. Eliashberg spectral function and electron-phonon coupling constant

The Eliashberg spectral function  $\alpha^2 F(\omega)$  and the electron-phonon coupling constant  $\lambda(\omega)$  are plotted as functions of the phonon energy  $\omega$  in Fig. 6. Superconductivity in these doped stanene systems is clearly in the intermediate coupling regime (i.e.,  $\lambda \sim 1$ ). The contributions to the EPC  $\lambda$  come from three main ranges of phonon energies: the low energy phonons with energies from 0 to  $\sim 60 \text{ cm}^{-1}$ , the intermediate energy phonons ( $\sim 80 - 150 \text{ K}$ ) and the ‘high’ energy regime ( $\gtrsim 150 \text{ K}$ ). For phonons with zero wavevector ( $\mathbf{q} = 0$ ), it is straightforward to determine which phonon modes correspond to each of these regimes. However, for those with  $\mathbf{q} \neq 0$ , it is difficult to unravel the phonon modes that contribute the most to a given phonon energy. Thus, it is difficult to determine the modes that enhance  $\lambda$  the most since all the wavevectors in the first Brillouin Zone contribute to the sum in Eq. 4. The interaction between the electrons and the low energy phonons contribute more than 70% to the EPC. The remaining  $\sim 30\%$  comes mainly from the electronic coupling with the intermediate energy phonons. In general, we expect that out-of-plane vibrational modes of stanene couples with the  $\pi^*$  and interlayer states to produce superconductivity in the doped system.

### B. Transition Temperature

Table II shows the results obtained from the calculations. We adopted a value of  $\mu^* = 0.13$  for the Coulombic repulsion parameter as this value reproduced, in a previous *ab initio* calculation,<sup>17</sup> the experimental  $T_c$  of bulk white Tin. Our results follow the trend of transition temperatures  $T_c$  observed by Profeta *et al.*<sup>5</sup> with regard to the ad atoms on a graphene sheet. That is, the ad atom that gives the highest  $T_c$  is the one whose height above the plane is smallest. From Table II, we see that the height  $\delta$  of the ad atom above the stanene plane is smaller for Lithium doped stanene  $\text{LiSn}_6$  than for its Calcium doped counterpart  $\text{CaSn}_6$

and, as expected,  $T_c$  for the former (1.3 K) is higher than that of the latter (0.7 K). One may argue that the value of the Coulomb repulsion parameter used in the bulk case might be different from that for the 2D system. In Fig. 7 we show the values of  $T_c$  determined for different values of  $\mu^*$  in the range from 0.1 to 0.2 as suggested in Ref. 18. The largest value of  $T_c$  obtained was 1.7 K (1.0 K) for  $\text{LiSn}_6$  ( $\text{CaSn}_6$ ). These values are significantly smaller than that predicted for Lithium-doped graphene (8.1 K), but agree with the low  $T_c$  value (1.4 K) for Calcium-doped graphene.<sup>5</sup>

In conclusion, we reported our results on phonon-mediated superconductivity in Lithium and Calcium doped stanene. We presented the electronic band structure, predicted the Eliashberg spectral function  $\alpha^2F(\omega)$ , and showed the contribution of the phonons to the total electron phonon coupling coefficient  $\lambda$ . Our results reveal that superconductivity can be induced in stanene by doping it with alkaline and alkaline earth atoms. We found that  $T_c$  for Lithium doped stanene should lie in the range from 0.48 to 1.70 K while that of the Calcium doped should lie somewhere from 0.15 to 1.04 K. These values of  $T_c$  are small, smaller than in the case for bulk  $\beta$ -Tin and Lithium-doped graphene. Further work should seek for methods to increase  $T_c$  either by straining stanene or/and by doping with other ad atoms.

#### IV. ACKNOWLEDGMENTS

YS is grateful to the African Development Bank (AfDB) for a scholarship. We thank the Abdus Salam International Center for Theoretical Physics (ICTP), Trieste, Italy for computer resources.

- 
- <sup>1</sup> S. Cahangirov, M. Topsakal, E. Aktuahin, and S. Ciraci, Phys. Rev. Lett. **102**, 236804 (2009).
  - <sup>2</sup> Y. Xu, B. Yan, H.-J. Zhang, J. Wang, G. Xu, P. Tang, W. Duan, and S.-C. Zhang, Phys. Rev. Lett. **111**, 136804 (2013).
  - <sup>3</sup> B. van den Broek, M. Houssa, E. Scalise, G. Pourtois, V. V. Afanas'ev, and A. Stesmans, 2D Mater. **1**, 021004 (2014).
  - <sup>4</sup> E. Margine and F. Giustino, Phys. Rev. B **90**, 014518 (2014).
  - <sup>5</sup> G. Profeta, M. Calandra, and F. Mauri, Nat. Phys. **8**, 131 (2012).
  - <sup>6</sup> C. Si, L. Zheng, D. Wenhui, and L. Feng, Phys. Rev. Lett. **111**, 196802 (2013).
  - <sup>7</sup> S.-L. Yang, J. Sobota, C. Howard, C. Pickard, M. Hashimoto, D. Lu, S.-K. Mo, P. Kirchmann, and Z.-X. Shen, Nat. Commun. **5**, 3493 (2014).
  - <sup>8</sup> J. Wang, Y. Xu, and S.-C. Zhang, Phys. Rev. B **90**, 054503 (2014).
  - <sup>9</sup> F. Zhu, W.-j. Chen, Y. Xu, C.-l. Gao, D.-d. Guan, C. Liu, D. Qian, S.-C. Zhang, and J.-f. Jia, ArXiv e-prints (2015), arXiv:1506.01601v1.
  - <sup>10</sup> J. P. Perdew, K. Burke, and M. Ernzerhof, Phys. Rev. Lett. **77**, 3865 (1996).
  - <sup>11</sup> P. Giannozzi, et. al., J. Phys. Condens. **21**, 395502 (2009).
  - <sup>12</sup> D. R. Hamann, M. Schluter, and C. Chang., Phys. Rev. Lett. **43**, 1494 (1979).
  - <sup>13</sup> S. Baroni, S. de Gironcoli, A. Dal Corso, and P. Giannozzi, Rev. Mod. Phys. **73**, 515 (2001).
  - <sup>14</sup> P. B. Allen and R. C. Dynes, Phys. Rev. B **12**, 905 (1975).
  - <sup>15</sup> P. Tang, P. Chen, W. Cao, H. Huang, S. Cahangirov, L. Xian, Y. Xu, S.-C. Zhang, W. Duan, and A. Rubio, Phys. Rev. B **90**, 121408 (2014).
  - <sup>16</sup> A. Fedorov, N. Verbitskiy, D. Haberer, C. Struzzi, L. Petaccia, D. Usachov, O. Vilkov, D. Vyalkikh, J. Fink, M. Knupfer, et al., Nat. Commun. **5**, 3257 (2014).
  - <sup>17</sup> Y. Shaidu, *Superconductivity of Tin and Doped Stanene*. Thesis, African University of Science and Technology, Abuja, Nigeria (2014).
  - <sup>18</sup> W. L. Mcmillan, Phys. Rev. **167**, 331 (1968).

Table I: Optimized lattice parameter of stanene:  $a$  is the lattice constant,  $d$  is the out-of-plane buckled height, and  $a_{sn-sn}$  is the  $Sn - Sn$  bond length; all distances are in Angstroms

|                                       | $a$  | $d$  | $a_{sn-sn}$ |
|---------------------------------------|------|------|-------------|
| This work                             | 4.64 | 0.92 | 2.84        |
| Broek <i>et al.</i> <sup>3</sup>      | 4.62 | 0.92 | 2.82        |
| Shou-Cheng <i>et al.</i> <sup>2</sup> | 4.65 | -    | -           |

Table II: Summary of results:  $\delta$  (in Å) is the height of the ad atom above the stanene plane,  $\omega_{log}$  (in K) is the logarithmic average of the phonon energy,  $\lambda$  is the electron-phonon coupling coefficient, and  $T_c$  (in K) is the transition temperature.

|                   | $\delta$ | $\omega_{log}$ | $\lambda$ | $T_c$ |
|-------------------|----------|----------------|-----------|-------|
| LiSn <sub>6</sub> | 1.75     | 60.97          | 0.65      | 1.3   |
| CaSn <sub>6</sub> | 2.24     | 62.62          | 0.54      | 0.7   |

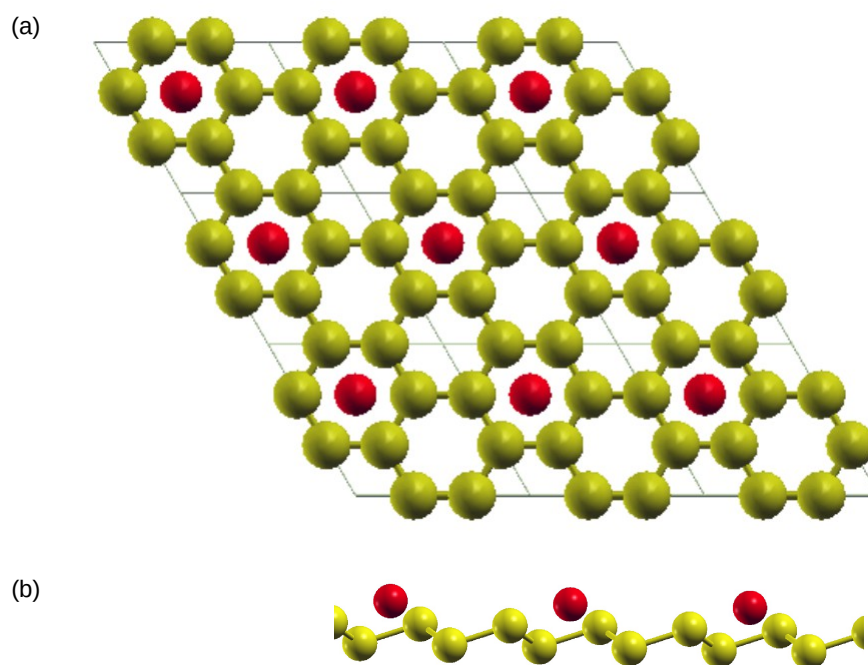


Figure 1: Crystal structure of doped stanene. The yellow spheres represent tin atoms while the red spheres are the dopants. Both the top (a) and the side views (b) are shown above and below, respectively.

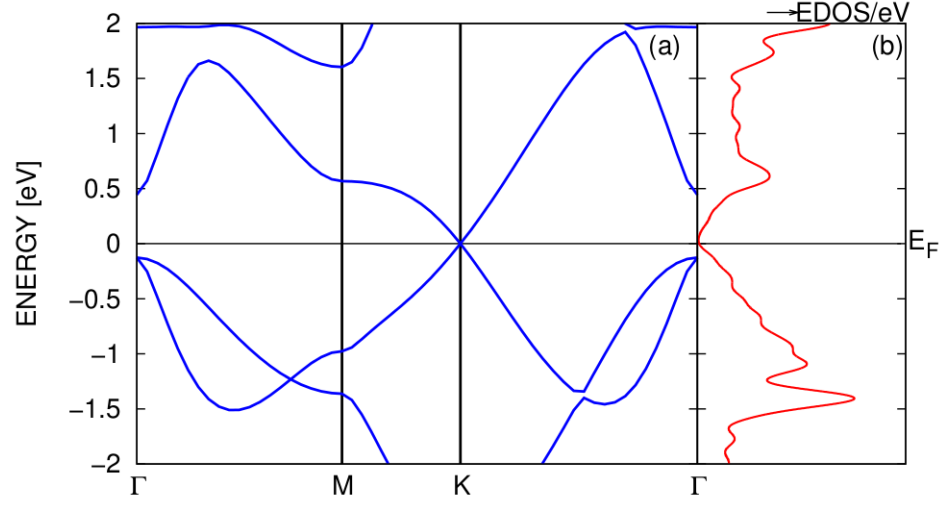


Figure 2: **(a)**, is the electronic band structure and, **(b)**, is the electronic density of states (EDOS) of stanene,  $E_F$  is the Fermi energy, which we set as the reference level, and  $\Gamma(0,0,0)$ ,  $M(\frac{1}{2},0,0)$ , and  $K(\frac{1}{3},\frac{1}{3},0)$  are special symmetry k points.

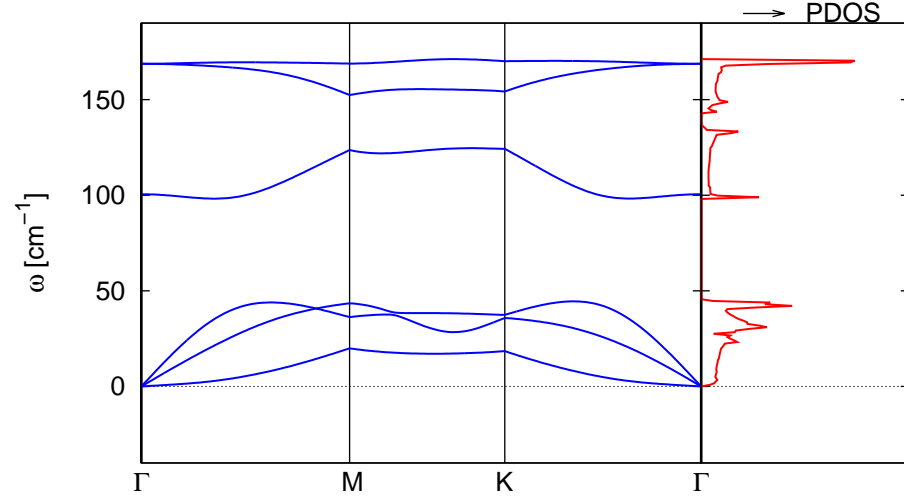


Figure 3: Phonon dispersion (left) and the phonon density of states (right) for buckled pristine stanene. The phonon dispersion is plotted along  $\Gamma$ ,  $M$ ,  $K$  and  $\Gamma$  high symmetry k points of a 2D honeycomb crystal

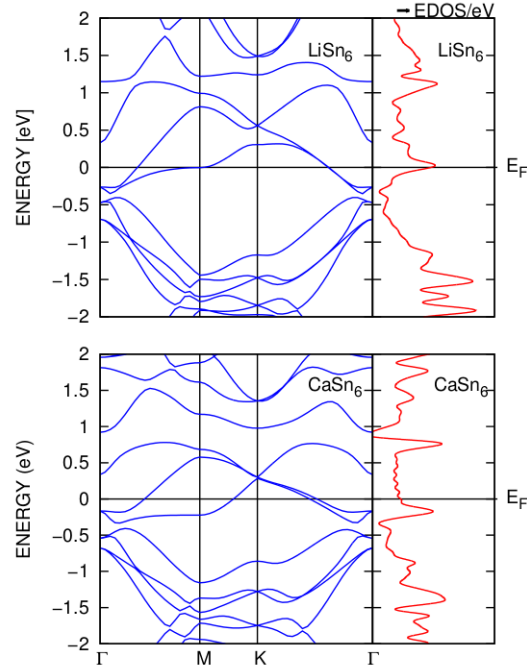


Figure 4: Electronic Band Structures and the Total Density of States. The top panel is for  $\text{LiSn}_6$  and the bottom one for  $\text{CaSn}_6$ . In each case, the electronic band structure is on the left while the total electronic density of states (EDOS) is on the right hand side.  $E_F$  is the Fermi energy, which we set as the reference level with a horizontal line. The band structure is plotted along the k-path connecting the  $\Gamma$ ,  $M$ ,  $K$  and  $\Gamma$  high symmetry k points of a 2D honeycomb crystal

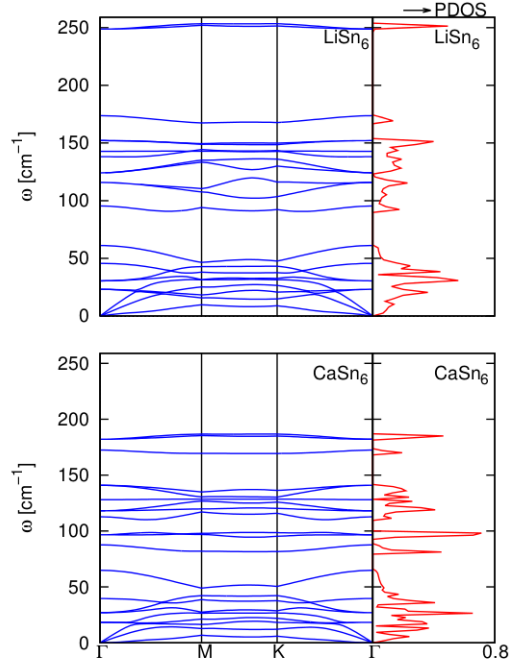


Figure 5: Phonon dispersion (left) and the phonon density of states (right) for Lithium-doped stanene,  $\text{LiSn}_6$  (top) and for Calcium-doped stanene,  $\text{CaSn}_6$  (bottom). The phonon dispersion are plotted along  $\Gamma$ ,  $M$   $K$  and  $\Gamma$  high symmetry k points of a 2D honeycomb crystal

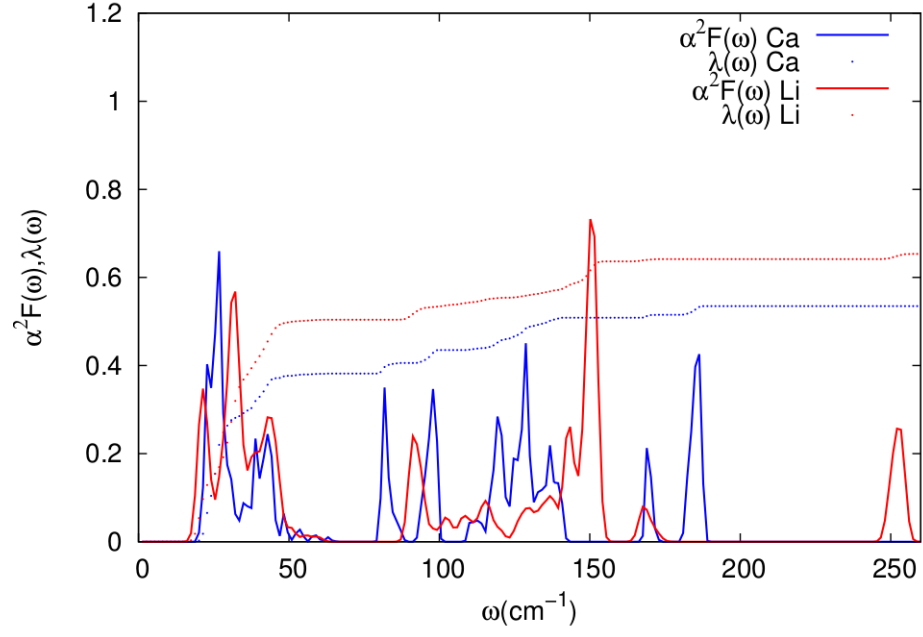


Figure 6: The Eliashberg spectral function  $\alpha^2 F(\omega)$  (solid lines) and the electron-phonon coupling constant  $\lambda(\omega)$  (dotted lines) for Lithium-doped and Calcium-doped stanene.

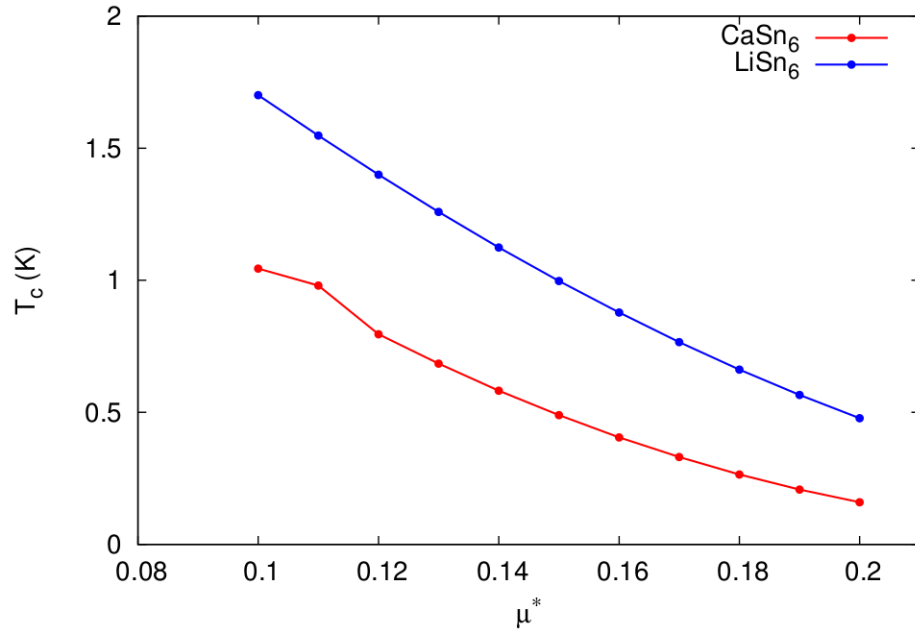


Figure 7: Transition Temperature  $T_c$  as a function of  $\mu^*$